Photosynthesis Research **66:** 33–44, 2000.

Emerging techniques

Short-pulse pump-and-probe technique for airborne laser assessment of Photosystem II photochemical characteristics

Alexander M. Chekalyuk[1,*], Frank E. Hoge[2], Charles W. Wright[2] & Robert N. Swift[3]
[1]*National Research Council;* [2]*Goddard Space Flight Center;* [3]*EG & G, Inc., NASA Goddard Space Flight Center, Wallops Flight Facility, Wallops Island, VA 23337, USA;* *Author for correspondence (e-mail: chekaluk@osb.wff.nasa.gov; fax: +1-757-824-1036)*

Received: 25 October 1999; accepted in revised form 31 August 2000

Key words: chlorophyll, fluorescence, LIDAR, photosynthesis, Photosystem II, pump and probe, remote sensing, singlet-singlet quenching, singlet-triplet quenching

Abstract

The development of a technique for laser measurement of Photosystem II (PS II) photochemical characteristics of phytoplankton and terrestrial vegetation from an airborne platform is described. Results of theoretical analysis and experimental study of pump-and-probe measurement of the PS II functional absorption cross-section and photochemical quantum yield are presented. The use of 10 ns probe pulses of PS II sub-saturating intensity provides a significant, up to 150-fold, increase in the fluorescence signal compared to conventional 'weak-probe' protocol. Little effect on the fluorescence yield from the probe-induced closure of PS II reaction centers is expected over the short pulse duration, and thus a relatively intense probe pulse can be used. On the other hand, a correction must be made for the probe-induced carotenoid triplet quenching and singlet-singlet annihilation. A Stern-Volmer model developed for this correction assumes a linear dependence of the quenching rate on the laser pulse fluence, which was experimentally validated. The PS II saturating pump pulse fluence (532 nm excitation) was found to be 10 and 40 μmol quanta m^{-2} for phytoplankton samples and leaves of higher plants, respectively. Thirty μs was determined as the optimal delay in the pump-probe pair. Our results indicate that the short-pulse pump-and-probe measurement of PS II photochemical characteristics can be implemented from an airborne platform using existing laser and LIDAR technologies.

Abbreviations: C_{A-} – proportion of closed ($P_{680}PheoQ_A^-$ state) photochemically active RC's ($0 < C_{A-} < 1$); C_T – proportion of carotenoid molecules in the triplet state ($0 < C_T < 1$); EEQ – excessive energy quenching; E and E_{pm} – probe and pump pulse fluences (μmol quanta m^{-2}), respectively; E_s – pulse fluence required to fully saturate PS II photochemistry; f – proportion of photochemically active RC's ($0 < f < 1$); Φ_F and Φ_P – actual Chl fluorescence and photochemical yields in PS II, respectively; Φ_m – maximum Chl fluorescence yield when all RC's are closed ($C_{A-} \cong 1$); Φ_o and Φ_{Po} – minimum fluorescence and maximum potential photochemical yields when all RC's are open ($C_{A-} \cong 0$); Φ_{oQ} and Φ_{mQ} – minimum and maximum fluorescence yields, respectively, in the EEQ excitation mode; $\Phi_{PoQ} \equiv (\Phi_{mQ} - \Phi_{oQ})/\Phi_{mQ}$ – relative pump-induced change in Chl fluorescence yield in the EEQ excitation mode; k_F – rate constant of Chl fluorescence in PS II; k_Σ – sum of all non-photochemical PS II rate constants (fluorescence, thermal dissipation, spillover to Photosystem I, etc); k_P – maximum potential rate constant of photochemical quenching in PS II; k_Q and k_{SSQ} – averaged over the pulse EEQ and SSQ rate parameters, respectively (the averaged EEQ and SSQ rate constants are equal to $k_Q E$ and $k_{SSQ}E$, respectively); k_{STQ} – STQ rate parameter at the end of the pulse; k_T – maximum potential STQ rate constant with all carotenoid molecules in the triplet state; P&P – pump and probe (technique); LIDAR – abbreviation of 'LIght Detection And Ranging', a laser remote sensing technique; $P_{680}^+PheoQ_A^-$ – intermediate RC state with oxidized pigment P_{680} and reduced quinone acceptor Q_A; $P_{680}PheoQ_A^-$ – closed RC state with re-reduced P_{680}^+ and reduced Q_A; Q_E – EEQ factor, see Equation (14); RC – PS II reaction center; $R_P = k_P/k_\Sigma$; $R_Q = k_Q/k_\Sigma$; $R_{SSQ} = k_{SSQ}/k_\Sigma$; $R_{STQ} =$

k_{STQ}/k_{Σ}; SP – short pulse ($\sim$ 10 ns); STQ and SSQ – singlet-triplet and singlet-singlet quenching, respectively; σ_{PSII} – PS II functional absorption cross-section; t – delay between pump and probe pulses in the pump-probe pair; τ_T and τ_{A-} – time constants of carotenoid triplet state decay and RC reopening, respectively

Introduction

During the past decade, a considerable emphasis within the remote sensing and marine biology communities has been focused on developing and improving algorithms for estimating oceanic primary productivity from satellite ocean color imagery (Hoge et al. 1999 and references cited therein). One of the major obstacles to achieving this capability is the high temporal and spatial variability in photosynthetic quantum yield among marine phytoplankton strains. There is currently no way to retrieve the information on the efficiency of light energy utilization directly from satellite ocean color imagery. The majority of techniques capable of measuring photosynthetic rate or quantum yield parameters must be conducted from a ship, which limits coverage for validation of satellite estimates of primary production. There is clearly a need for a technology capable of filling the spatial/temporal gap between satellite and shipboard measurements to provide more accurate estimates of phytoplankton photosynthesis and abundance.

The airborne approach to meet this demand can rely on recent advances in active fluorosensing of photosynthesizing organisms. Fluorescence 'pump-and-probe'(P&P) (Mauzerall 1972; Falkowski et al. 1986; Kramer et al. 1990; Chekalyuk and Gorbunov 1994), 'fast-repetition-rate' (Falkowski and Kolber 1995; Kolber et al. 1998), 'pulse-amplitude-modulation' (Schreiber et al. 1993; Hofstraat et al. 1994), and 'pump-during-probe' (Olson et al. 1996; Chekalyuk et al. 1997; Olson et al. 1999) techniques are currently in use in shipboard and laboratory settings to monitor phytoplankton photochemical parameters. The basic concept is to saturate the photochemical activity within PS II reaction centers (RC's) with a light flash (or series of 'flashlets') while measuring a corresponding induction rise in the quantum yield of chlorophyll (Chl) fluorescence (Govindjee 1995; Kramer and Crofts 1996).

Since its introduction in the 1970s (Kim 1973), LIDAR-fluorosensor techniques have matured from a research area into a useful operational tool for ecological and biological surveying over large aquatic areas (e.g. see Hoge 1988; Chekalyuk et al. 1995). Chl fluorescence can be routinely monitored by airborne LIDAR. The conversion of these laser-induced Chl fluorescence measurements into absolute units of Chl concentration and phytoplankton abundance, however, is complicated because of variability in the quantum yield of Chl fluorescence (Falkowski and Kolber 1995). This variability is caused, to a large extent, by changes in PS II photochemical efficiency under varying environmental conditions. The development of an advanced LIDAR-fluorosensor capable of assaying photochemical parameters along with conventional fluorescence monitoring would improve the accuracy of 'traditional' LIDAR-based estimates and provide valuable information on phytoplankton photosynthetic activity.

The first shipboard (Chekalyuk and Gorbunov 1994) and airborne (Johnson et al. 1995) tests of P&P LIDAR prototypes proved the feasibility of the approach, but these proof-of-concept experiments also emphasized the sensitivity limitation of the P&P technique as the major obstacle for its operational implementation from an airborne platform. Utilization of intense laser pulses can provide an acceptable signal/noise ratio for LIDAR measurement from an airborne platform flying at a reasonable altitude. On the other hand, such pulses may cause RC closure potentially affecting the accuracy of P&P measurement, and produce excessive energy quenching (EEQ) through singlet–triplet and singlet-singlet mechanisms (Breton et al. 1979; Mathis et al. 1979). EEQ conversion of excitation energy into heat causes a decline in the yields of Chl fluorescence (Bunin et al. 1992) and PS II photochemistry as competitive energy dissipation mechanisms, and may also result in less-efficient RC blocking by the saturating pump pulse (Rosema and Zahn 1997). The experimental data must, therefore, be corrected to retrieve 'original' PS II fluorescence and photochemical characteristics. The goals of the research reported here were to develop and experimentally verify a simplified, yet adequate biophysical model to account for effects of intense short-pulse excitation, and to optimize laser excitation for airborne P&P LIDAR measurements.

Chl fluorescence and photochemical quantum yields

The active fluorescence techniques for assessment of the PS II photochemical characteristics are based on the competing relationship (Krause and Weis 1991;

Govindjee 1995) between Chl fluorescence and photochemical light energy utilization in PS II. Assuming a high connectivity between RC's and a rapid equilibration of excitation within the PS II light harvesting antenna, the quantum yields of Chl fluorescence Φ_F and PS II photochemistry Φ_P can be respectively expressed as

$$\Phi_F = k_F/(k_\Sigma + (1 - C_{A-}) \cdot f \cdot k_P), \quad (1)$$

and

$$\Phi_P = (1 - C_{A-}) \cdot f \cdot k_P/ (k_\Sigma + (1 - C_{A-}) \cdot f \cdot k_P). \quad (2)$$

Here, k_F is a fluorescence rate constant, k_Σ is a sum of all non-photochemical PS II rate constants (fluorescence, thermal dissipation, spillover to Photosystem I, etc.); f is a proportion of the functional RC's (Greene et al. 1992); and C_{A-} is a proportion of functional RC's in the 'closed' $P_{680}PheoQ_A^-$ state (Krause and Weis 1991). C_{A-} depends on the intensity of incident light and can vary in value between 0 and 1. f can also vary in a range of 0–1 depending on environmental factors such as nutrient supply (Greene et al. 1992; Falkowski and Kolber 1995). k_P is the maximum potential rate constant of photochemical charge separation in PS II when all the RC's are functional and open.

In the dark-adapted state, when all RC's are open ($C_{A-} = 0$), the fluorescence yield is minimal:

$$\Phi_o = k_F/(k_\Sigma + f \cdot k_P), \quad (3)$$

while Φ_P reaches its maximum potential value in the current PS II photochemical functional state f:

$$\Phi_{Po} = f \cdot k_P/(k_\Sigma + f \cdot k_P). \quad (4)$$

The maximal Φ_{Po} magnitudes were found to be 0.65 (Falkowski and Kolber 1995) and 0.83 (Krause and Weis 1991) for phytoplankton and higher plants, respectively. Using these values and assuming $f = 1$ in Equation (4), the ratios $R_P = k_P/k_\Sigma$ can be then respectively estimated as 1.86 (phytoplankton) and 4.95 (higher plants). Equation (4) can be transformed to a convenient parameterized form:

$$\Phi_{Po} = f \cdot R_P/(1 + f \cdot R_P). \quad (5)$$

When all RC's are closed ($C_{A-} = 1$), the PS II photochemistry is blocked ($\Phi_P = 0$ in Equation (2)) and the Chl fluorescence yield is maximal:

$$\Phi_m = k_F/k_\Sigma \quad (6)$$

From Equations (3), (4), and (6):

$$\Phi_{Po} = (\Phi_m - \Phi_o)/\Phi_m. \quad (7)$$

Equation (7) relates the relative change in Chl fluorescence yield, $(\Phi_m - \Phi_o)/\Phi_m$, and photochemical quantum yield (Genty et al. 1989; Krause and Weis 1991; Govindjee 1995). It is widely used for estimating PS II photochemical efficiency based on measurements of variable fluorescence, $\Phi_m - \Phi_o$.

Pump-and-probe technique

The conventional P&P protocol (left panel in Figure 1) is based on the use of a 'pump' pulse to initialize a transition of a fraction of RC's to the closed $P_{680}PheoQ_A^-$ state. The corresponding change in the fluorescence yield is measured using a weak probe pulse that follows the pump pulse by a delay t. In the 1–100 μs delay time interval, pump-induced carotenoid singlet–triplet quenching (STQ) (Mathis et al. 1979; Breton et al. 1979) also affects fluorescence yield, therefore the post-pump transition of fluorescence quantum yield in this interval can be presented as:

$$\Phi_F(t) = k_F/(k_\Sigma + (1 - C_{A-}\exp(-t/\tau_{A-})) \cdot f \cdot k_P + k_T C_T \exp(-t/\tau_T)). \quad (8)$$

Here, C_T is the proportion of carotenoid molecules in the triplet state at the end of the pump pulse ($0<C_T<1$), k_T is the maximum potential STQ rate constant, τ_{A-} and τ_T are time constants of RC reopening and triplet decay, respectively. From Equations (8), (3) and (4) it follows that:

$$(\Phi_F - \Phi_o)/\Phi_F = \Phi_{Po} C_{A-} (\exp(-t/\tau_{A-}) - (k_T C_T/f \cdot k_P C_{A-}) \cdot \exp(-t/\tau_T)). \quad (9)$$

The closing of dark-adapted RC's by a short (<1 μs) actinic flash can be well described (e.g. see Vulkunas et al. 1991) by:

$$C_{A-} = 1 - \exp(-\sigma_{PSII} E_{pm}). \quad (10)$$

Here, σ_{PSII} is a PS II functional absorption cross-section, and E_{pm} is the pump pulse fluence. The pump-induced carotenoid triplet states decay at the delay time $t \sim 2 \ln 10\, \tau_T$ while the magnitude of $\exp(-t/\tau_{A-})$ is still close to 1 ($\tau_{A-} >> \tau_T$) and, therefore, $(\Phi_F - \Phi_o)/\Phi_F \cong \Phi_{Po} \cdot C_{A-}$ in Equation (9). This and the use of Equation (10) results in:

$$(\Phi_F - \Phi_o)/\Phi_F \cong \Phi_{Po}(1 - \exp(-\sigma_{PSII} E_{pm})). \quad (11)$$

Equation (11) is the basic equation of the P&P technique. If the pump pulse is strong enough to close most

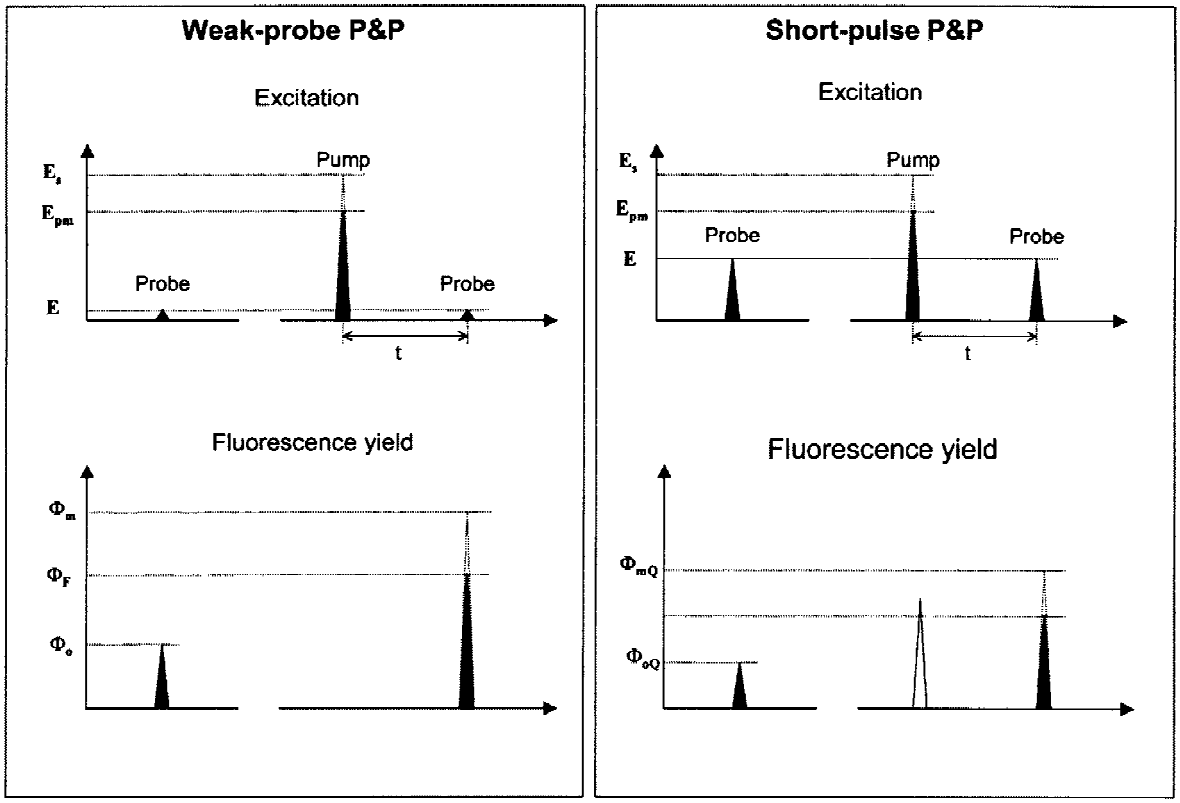

Figure 1. Diagram of the weak-probe (left panel) and short-pulse (right panel) pump-and-probe protocols for measurement of PS II photochemical parameters. Both protocols are based on measuring the relative change in Chl fluorescence yield caused by the PS II saturating pump pulse at a delay time, *t*, after its action. The use of a sub-saturating 10 ns probe pulse in the SP-P&P protocol provides up to a 150-fold increase in sensitivity, but requires a correction for excessive energy quenching. Pump-induced Chl fluorescence (blank triangle in the right panel) can be used to retrieve correction parameters.

of the RC's ($E_{pm} \cong E_s$, left panel in Figure 1), $\Phi_F \cong \Phi_m$ and $(\Phi_F - \Phi_o)/\Phi_F$ is a good estimate for the potential PS II photochemical yield Φ_{Po} in accordance with Equation (7). Such a 'saturating' fluence magnitude E_s can be assessed from Equation (10) as $4.6\sigma_{PSII}^{-1}$ (C_{A-} = 0.99). Performing a best fit of Equation (11) to the measured $(\Phi_F - \Phi_o)/\Phi_F$ dependence on E_{pm} in the sub-saturating fluence range yields the magnitude of σ_{PSII}, another important PS II parameter. The closer the $(\exp(-t/\tau_{A-}) - (k_T C_T/f \cdot k_P C_{A-}) \cdot \exp(-t/\tau_T))$ value in Equation (9) is to 1, the higher the accuracy of the estimate. In practice, the P&P underestimation of Φ_{Po} is in the range of few percent due to partial reopening of pump-closed RC's (see 'Discussion').

Short-pulse pump-and-probe protocol

The 'weak-probe' condition (Falkowski et al. 1992; Kolber et al. 1998) of the conventional P&P protocol assumes that the pulse should not significantly affect the Chl fluorescence yield, i.e. it should close less than 1% of the RC's. A 'weak' probe fluence level can therefore be estimated as $10^{-2}\sigma_{PSII}{}^{-1} \cong E_s/500$. The restriction imposed on the probe pulse results in a potentially weak probe-induced Chl fluorescence response. The laser used in the NASA Airborne Oceanographic LIDAR provides a reasonable signal/noise ratio in laser-induced Chl fluorescence signal from an operational altitude of 150 m with a pulse energy of ~100 mJ. Our measurements indicate that the corresponding in-water excitation pulse fluence reaches the PS II saturating magnitude $E_s \sim 10$ μmol quanta m^{-2}. Modifying the system to meet the 'weak-probe-pulse' requirement of the P&P protocol (i.e. maintaining a 500-fold difference between the pump and probe fluence) would require either (i) a 20-fold increase in the beam diameter of the existing probe laser along with the use of a pump laser of 50 J pulse energy, or (ii) the use of the existing laser as a pump laser in conjunc-

tion with a probe laser of 0.2 mJ pulse energy. The first option is practically impossible. The second one, which would require a 500-fold decrease in excitation intensity compared to the current system configuration, would result in an unacceptable signal/noise ratio in fluorescence response. Thus, the use of a PS II sub-saturating probe pulse seems to be inevitable in an airborne P&P LIDAR.

According to our analysis, a probe pulse of 10 ns width can be of sufficient energy density to eventually close a substantial portion of the RC's, but probe-induced changes in the RC state *during the pulse* should not noticeably affect the P&P estimate of PS II photochemical yield. Indeed, exciton trapping by initially open RC's causes a fast (sub-ns time scale) transition into the intermediate state $P_{680}{}^{+}PheoQ_A{}^{-}$ (Krause and Weis 1991), which has about the same trapping efficiency as the open RC state (Deprez et al. 1983; Bunin et al. 1992). The time constant of further transition to the closed state $P_{680}PheoQ_A{}^{-}$ is in the range of 28–300 ns or longer (Deprez et al. 1983; Schlodder et al. 1984). Therefore, the probe-induced fraction of RC's actually transferred to the $P_{680}PheoQ_A{}^{-}$ state during the 10 ns sub-saturating pulse is too small to noticeably change the PS II energy balance and Chl fluorescence yield. According to our assessment, based on data presented in (Schlodder et al. 1984), even the use of a PS II saturating probe pulse would result in less than a 3% overestimation in the original fluorescence yield Φ_o. Regarding Φ_m measurement, note that the preceding pump pulse has already closed most of the RC's. Therefore, the delayed probe pulse would not change their state regardless of its intensity. Thus, the 'weak-pulse' restriction in terms of 'non-closing' RC's can be eliminated in the case of sub-10 ns probe pulses and the use of intensive sub-saturating (0.1–15 μmol quanta m^{-2}) probe pulses may provide a significant increase in the response signal.

Excessive energy quenching

Generally, both SSQ and STQ rates are non-linear with respect to excitation intensity (Breton et al. 1979; Rosema and Zahn 1997). Nonetheless, as with any non-linear function, they can be approximated by linear dependencies within some limited intensity range. The experimentally observed linear dependencies of the reciprocal of the fluorescence and photochemical yields on the probe pulse fluence in the PS II sub-saturating range (for example, see Figure 6, which will be discussed later) suggest that a simple Stern–Volmer-type model (e.g. Karukstis et al. 1987) is applicable to describe the overall quenching effect. Equations for photochemical and fluorescence yields in the EEQ mode can therefore be derived by adding the EEQ rate constant $k_Q \cdot E$ to the denominators of Equations (1)–(4) and (6). In particular, the original (Φ_{oQ}) and maximum (Φ_{mQ}) fluorescence yields in the presence of EEQ can be expressed as:

$$\Phi_{oQ} = k_F/(k_\Sigma + f \cdot k_P + k_Q \cdot E) \quad \text{and}$$
$$\Phi_{mQ} = k_F/(k_\Sigma + k_Q \cdot E). \qquad (12)$$

According to the above discussion, we can neglect to a first approximation the formation of the closed RC state $P_{680}PheoQ_A{}^{-}$ during the 10 ns sub-saturating probe pulse, so $f \cdot k_P$ describes the overall excitation trapping by both open and probe-induced intermediate $P_{680}{}^{+}PheoQ_A{}^{-}$ states. Similar to Equation (7), one can derive from Equation (12):

$$\Phi_{PoQ} = (\Phi_{mQ} - \Phi_{oQ})/\Phi_{mQ} = f \cdot R_P/(1 + f \cdot R_P + R_Q \cdot E). \qquad (13)$$

Here, $R_Q = k_Q/k_\Sigma$. The product $R_Q \cdot E$ characterizes the ratio of the EEQ rate to the overall rate of non-photochemical energy quenching in the low-excitation mode. Note that a decrease in the quenching rate, $R_Q \cdot E$, results in transforming Equation (13) into Equation (5), which describes the PS II photochemical yield, Φ_{Po}.

The EEQ effect can be quantitatively described by the quenching factor Q_E. From Equations (3), (5) and (12)–(13), both the original fluorescence and photochemical yields must be equally quenched at any given excitation intensity in a sub-saturating EEQ probe mode:

$$Q_E = \Phi_{Po}/\Phi_{PoQ} = \Phi_o/\Phi_{oQ} = 1 + R_Q \cdot E/(1 + f \cdot R_P). \qquad (14)$$

A correction procedure can be applied to calculate the magnitude of the low-light photochemical quantum yield, Φ_{Po}, based on the measured magnitude of the 'quenched' fluorescence parameter, Φ_{PoQ}. A correction formula is derived from Equations (5) and (14):

$$\Phi_{Po} = (1 + R_Q \cdot E)/(\Phi_{PoQ}^{-1} + R_Q \cdot E). \qquad (15)$$

STQ and SSQ contributions to the overall EEQ effect

Estimates of individual STQ and SSQ rate paramet-

ers and their relative contributions to EEQ help in the optimization of the SP-P&P experimental protocol, particularly in selecting the pulse duration. The overall STQ effect depends on the pulse-induced concentration of carotenoid triplets, C_T, which was found to be identical for picosecond pulse trains and microsecond pulse in the PS II saturating fluence range (Breton et al. 1979). The instantaneous SSQ rate is dependent on the square of the exciton concentration in the light-harvesting antenna (e.g. see Breton et al. 1979; Bunin et al. 1992; Rosema and Zahn 1997). Therefore, the SSQ effect should quickly decline with increasing pulse duration at a fixed fluence, while the STQ must remain of the same order of magnitude.

For evaluation purposes, let us consider a few-ns actinic flash of sub-saturating (or saturating) fluence E that causes both STQ and SSQ. A linear rise of carotenoid triplet concentration was observed over a fluence range up to 250 μmol quanta m^{-2} (e.g. see Figure 3 in Breton et al. (1979). Therefore, a linear dependence $k_{STQ} \cdot E$ can be a reasonable approximation for the STQ rate, $k_T C_T$, in a PS II sub-saturating fluence range $E < 15$ μmol quanta m^{-2}. Equation (9) can then be transformed to a parameterized form:

$$(\Phi_F - \Phi_o)/\Phi_F = (f \cdot R_P \cdot C_{A-} \cdot \exp(-t/\tau_{A-}) - R_{STQ} \cdot E \cdot \exp(-t/\tau_T))/(1 + f \cdot R_P). \quad (16)$$

Here, $R_{STQ} = k_{STQ}/k_\Sigma$. Pump-induced SSQ is not included in Equations (9) and (16), since the exciton concentration and SSQ, respectively, decline at sub-ns scales during extinguishing excitation. Equation (16) provides a basis for assessing a number of parameters, including the R_{STQ} ratio, τ_T, and τ_{A-}. Due to a linear rise, the STQ rate constant averaged over the pulse duration must be equal to half of the one at the end of the pulse, i.e. $0.5 \cdot k_{STQ} \cdot E$. The observed linear rise in the overall EEQ effect (e.g. see Figure 6) suggests a linear dependence of the SSQ rate on E, and the overall EEQ rate can be presented then as $k_Q \cdot E = (k_{SSQ} + 0.5 \cdot k_{STQ}) \cdot E$. Here, k_{SSQ} is an SSQ rate parameter. Therefore, the relative SSQ rate parameter $R_{SSQ} = k_{SSQ}/k_\Sigma$ can be estimated as:

$$R_{SSQ} = R_Q - 0.5 \cdot R_{STQ} \quad (17)$$

Experimental setup and materials

A schematic of the lab-built double-pulse laser fluorometer is presented in Figure 2. It includes two Nd:YAG lasers (CFR 400, Big Sky Laser Technologies, 8.5 ns pulse duration, max pulse energy 135 mJ at 532 nm), a 99% dielectric folding mirror (Newport), a 50% beam splitter/mixer (Melles Griot), and a 4× beam expander (lab-made). The power of the probe pulse from Laser 2 was adjusted through a combination of neutral density filters and computer control of the laser power supply. A thin glass beam sampler reflected a small portion of the beams to a photodiode (Hamamatsu) for monitoring laser output energy. A gaussian compensator (Optics for Research) homogenized the energy distribution in the cross sections of both laser beams. A phytoplankton sample in the cylindrical glass cell (or a leaf attached to the sample holder) was placed in front of the focusing lens (f = 100 mm, D = 60 mm, Melles Griot) used for fluorescence collection. A black box (not shown in Figure 2) was placed over the sample holder to provide isolation from the ambient light. A laser power meter (H310, Scientech), mounted behind the sample holder, provided data for calculation of excitation fluence. A photomultiplier tube (PMT) module (HC125, Hamamatsu) was placed normal to the path of the laser excitation beam to measure the chlorophyll fluorescence from the sample through a

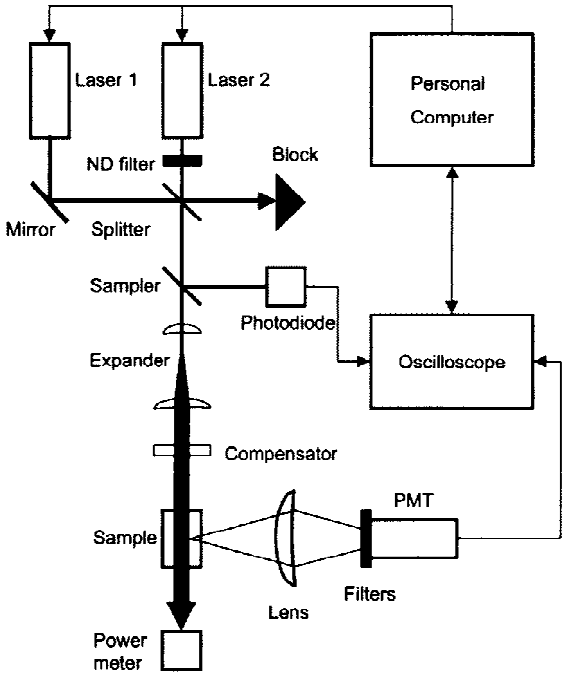

Figure 2. Schematic of the double-pulse laser fluorometer used to perform the SP-P&P laboratory experiments (see description in the text).

band-pass interference filter (700/70 nm, Intor) and removable neutral density (Melles Griot) filters.

The PMT module included a built-in preamplifier (8 MHz bandwidth) and a high-voltage power supply. Chlorophyll excitation was provided using single probe pulses and pump-probe pairs (see Figure 1) alternately applied to the sample at a repetition rate of 0.5 Hz. The delay between pump and probe pulses in the pump-probe pair could be varied over a range of 1 – 100 μs. A personal computer (PC) was used to control the operation of the laser power supplies and the PMT gain. The laser pulses were triggered with a multifunctional PC board (PCI-20428W-1A, Intelligent Instrumentation). The analog signals from the PMT and photodiode were routed into a 2-channel digital oscilloscope (model 9450, LeCroy) and the output was transferred to the PC through a GPIB-488 interface. The software for data acquisition and hardware control was developed using a 'Visual Designer 4.0' application generator package (Intelligent Instrumentation). Data processing, including non-linear regression fitting, was accomplished using 'Axum 5' (MathSoft) software.

Batch cultures of the diatom *Thalassiosira weissflogii* and the flagellate *Pleurochrysis carterae* were grown in an *f*/2 medium (Guillard 1975) at 20 °C under continuous illumination ('cool-white' fluorescent, ~100 μmol quanta $m^{-2}s^{-1}$). The P&P measurements were conducted with samples taken at different culture ages. Surface seawater samples of 250 ml were taken in the Middle Atlantic Bight in June–July 1998. Though the major focus of our investigation was on studying marine phytoplankton, measurements with leaves of *Fagus grandifolia* were conducted to provide data for further optimization of LIDAR P&P measurement of terrestrial vegetation.

Experimental methods and results

'P&P vs. Pump' measurements

Knowledge of the PS II saturating fluence $E_s = 4.6 \cdot {\sigma_{PSII}}^{-1}$ and its potential variability is a critical factor in the optimization of airborne SP-P&P protocol. The σ_{PSII} magnitudes were assessed along with Φ_{Po} values by best fitting with Equation (11) to measured $(\Phi_F - \Phi_o)/\Phi_F$ dependencies on the pump fluence ('P&P vs. Pump' protocol). During the experiment the pump fluence was varied within a range of 0.7–50 μmol quanta m^{-2} (phytoplankton) or 0.7–100 μmol quanta m^{-2} (leaves), while the probe pulse

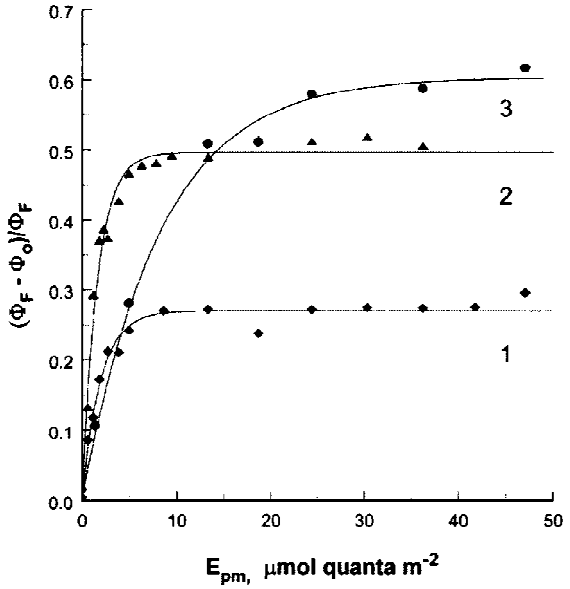

Figure 3. Chl fluorescence induction with increasing the actinic pump pulse fluence E_{pm} measured with the 'P&P vs. Pump' protocol. (1) sample of seawater; (2) *P. carterae*, (3) leaf of *F. grandifolia*. Measurements obtained during the experiment are shown as discrete points. The solid lines are plots of curves generated from a non-linear regression of the points with Equation (11).

fluence was fixed at 0.08 μmol quanta m^{-2} to minimize the EEQ effect. The delay t in the pump-probe pair was 30 μs. Typical results for phytoplankton (curves 1, 2) and leaves of *Fagus grandifolia* (curve 3) are presented in Figure 3. The horizontal axis of Figure 3 (and other plots to follow) is scaled in absolute pulse flux units obtained through calibration of the laser excitation energy with a laser power meter. The solid lines represent non-linear regression fitting of the experimentally determined points (symbols) using Equation (11). The retrieved σ_{PSII} and Φ_{Po} parameters are presented in the 'P&P vs. Pump' column of Table 1.

'P&P vs. Probe' measurements

Verification of the theoretical model and assessment of the magnitude, species and functional variability of the overall EEQ effect were conducted by measuring the Φ_{PoQ} dependence on the probe fluence with the pump fluence fixed at the PS II saturating level ('P&P vs. Probe' protocol). A non-linear regression of the fluorescence measurements with Equation (13) provided magnitudes for the R_Q and f parameters. The Φ_{Po} magnitude was estimated by using Equation (5). In this experiment series, the pump fluence was fixed at

Table 1. Magnitudes of PS II photochemical, absorption and quenching parameters estimated based on experimental measurements for phytoplankton cultures, seawater samples and leaves of *Fagus grandifolia.* Results obtained in the 'P&P vs. Pump', 'P&P vs. Probe', and 'P&P vs. Delay' experiments are presented in corresponding columns. The $R_{SSQ}/0.5\ R_{STQ}$ parameter reflects the relative contributions of singlet–singlet and singlet–triplet quenching mechanisms (SSQ and STQ, respectively) to the overall EEQ rate, $k_Q E$, under 10 ns pulse excitation at 532 nm

Species and samples examined	'P&P vs. Pump'		'P&P vs. Probe'		'P&P vs. Delay'			$R_{SSQ}/0.5\ R_{STQ}$
	σ_{PSII}, 10^{-15} cm^2	Φ_{Po}	R_Q, μmol^{-1} quanta m^2	Φ_{Po}	0.5 R_{STQ}, μmol^{-1} quanta m^2	Φ_{Po}	τ_T, μs	
T. weissflogii	12	0.55	0.43	0.60	0.12	0.56	4.2	
	8.2	0.16	0.45	0.19	0.11	0.57	5.7	2.9
P. carterae	11	0.50	0.20	0.51	0.012	0.55	7.3	16
Seawater	9.0	0.27	0.44	0.53	0.018	0.58	4.5	22
sample			0.40	0.38				
Fagus grandifolia	2.0	0.60	0.12	0.65	0.012	0.55	4.2	9

44–53 μmol quanta m^{-2} for excitation of phytoplankton and leaves of higher plants, respectively. Plots showing the Φ_{PoQ} dependence on the probe pulse fluence, which was varied within a range of 0.17–30 μmol quanta m^{-2}, are presented in Figure 4. The solid lines represent non-linear regression fitting of the experimentally determined points (symbols) using Equation (13). Estimated magnitudes of the EEQ relative rate parameter, R_Q, and the PS II photochemical yield, Φ_{po}, are presented in the 'P&P vs. Probe' column of Table 1.

'P&P vs. Delay' measurements

The following procedure was applied to assess the individual STQ and SSQ contributions to the overall EEQ effect. The $(\Phi_F - \Phi_o)/\Phi_F$ dependence on the delay time, t, between the pump and probe pulses were measured by using a 'P&P vs. Delay' protocol similar to that used in (Mauzerall 1972). In this procedure, a saturating (or sub-saturating) pump pulse of fixed intensity was used in combination with a weak probe pulse of fixed intensity while the delay in the pump-probe pair was varied within a range of 4–90 μs (see left panel in Figure 1). A non-linear regression of the experimentally determined data points using Equation (16) revealed the magnitudes of R_{STQ}, τ_T, τ_{A-}, and f. The magnitude of pump-closed RC fraction, C_{A-}, was calculated using Equation (10) and the σ_{PSII} value measured in the 'P&P vs. Pump' experiment. The R_{SSQ} parameter was then estimated using Equation (17) and the R_Q value derived from 'P&P vs. Probe' measurement. The pump pulse fluences were fixed at different sub-saturating and saturating magnitudes (1.7–50 μmol quanta m^{-2}) in different experimental series, which helped to verify the validity of Equation (16) in this fluence range. The probe pulse fluence was fixed at 0.08 μmol quanta m^{-2}. Examples of measured $(\Phi_F - \Phi_o)/\Phi_F$ dependencies on t can be seen in Figure 5 and magnitudes of the retrieved 0.5 R_{STQ} and Φ_{Po} parameters are presented in the 'P&P vs. Delay' column of Table 1. Φ_{Po} values were calculated based on f magnitudes and Equation (5). The τ_{A-} estimates were found to be in a range of 0.43–2 ms, which is consistent with data presented in the literature (e.g. see Krause and Weis 1991; Govindjee 1995), see also related references in Olson et al. 1996).

Discussion

In the 'P&P vs. Probe' investigation, a linear rise of $\Phi_{PoQ}{}^{-1}$ with increasing probe pulse fluence (within the PS II sub-saturating range) was found for all samples examined. This trend is clearly in evidence in Figure 6 where two experimental dependencies are plotted as a function of pulse fluence. This finding confirms the applicability of the Stern–Volmer model (Equations (13, 14)) to describe EEQ effect within this range. A pronounced decline in Φ_{PoQ} with increasing probe pulse intensity was observed for all samples in the 'P&P vs. probe' experiment (see Figure 4). The R_Q values given in Table 1 can be used to quantitatively estimate the EEQ effect using Equation (14) for any

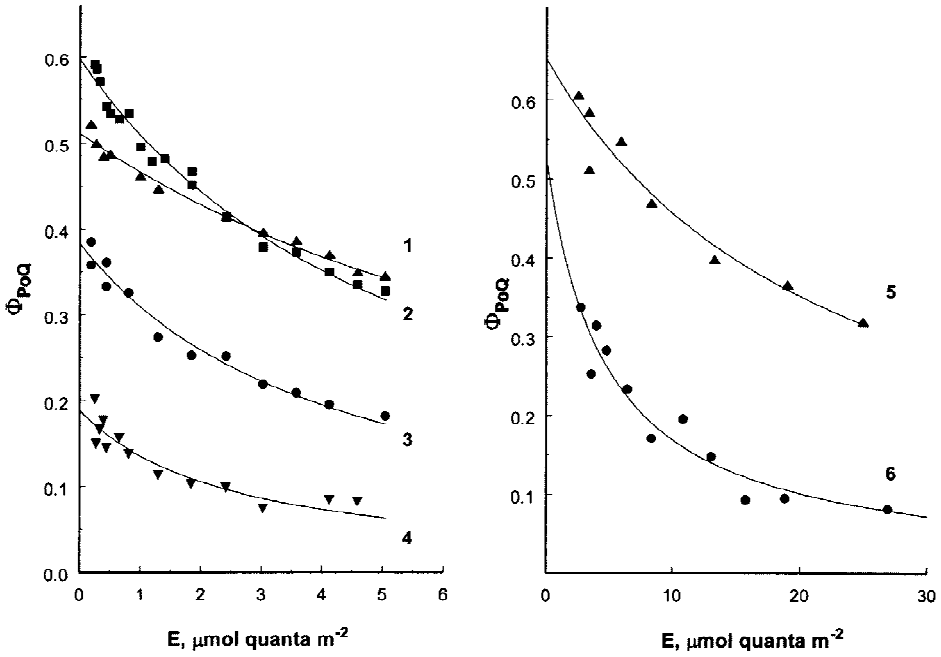

Figure 4. EEQ decline in Φ_{PoQ} with increasing probe pulse fluence E_p measured with the 'P&P vs. Probe' protocol. Measurements obtained from *P. carterae* (1), *T. weissflogii* (2, 4), seawater samples (3, 6), and leaf of *F. grandifolia* (5) are shown as discrete points. The solid lines are plots of curves generated from a non-linear regression of the points with Equation (13).

given PS II photochemical efficiency and excitation intensity. For example, a quenching factor $Q_E = 2.8$ can be calculated for a PS II saturating fluence $E_s = 4.6 \cdot \sigma_{PSII}{}^{-1} = 8.5$ μmol quanta m^{-2} for a seawater sample assuming a moderate PS II photochemical efficiency ($f = 0.5$) and a seawater-mean value of $R_Q = 0.42$ μmol^{-1} quanta m^2 as presented in Table 1. The EEQ effect would become negligible ($Q_E < 1.01$) at excitation fluences lower than 0.04 μmol quanta m^{-2}, which is of the same order of magnitude as the 'weak-probe' fluence, $10^{-2}\sigma_{PSII}{}^{-1} = 0.02$ μmol quanta m^{-2}. As predicted by the theoretical analysis, EEQ was found to be more pronounced (see data for the *T. weissflogii* species in Figure 4) in the case of poor photochemical efficiency (i.e. low f in Equation (14)), while the EEQ relative rate parameter, R_Q, *per se* did not indicate significant changes with variations in PS II photochemical efficiency (see Table 1). Generally, the EEQ effect was found to be well pronounced over the PS II sub-saturating range and should be taken into account when interpreting SP-P&P measurements.

A comparison of data obtained using 'P&P vs. Probe' protocol with observations acquired using the 'P&P vs. Delay' protocol provides useful information about the SSQ and STQ contributions to the EEQ effect. The magnitudes of the $R_{SSQ}/0.5\ R_{STQ}$ ratio determined by using Equation (17) are presented in the right-hand column of Table 1. These data indicate that SSQ was the dominant EEQ mechanism at 10 ns pulse excitation within the sample group examined and showed that the SSQ/STQ rate ratio varied between 2.9 and 22. The SSQ component and, therefore, the overall EEQ effect did not show strong species variability within the phytoplankton group ($\sim$2-fold variation range in R_Q), while the STQ rate and its relative contribution varied by a factor of 10. The observed higher STQ variability can be potentially caused by variations in carotenoid concentration between species. In terms of airborne LIDAR measurements in the ocean, a 10 ns pulse duration would be expected to result in less variation in the EEQ effect compared to a 100 ns pulse duration where the STQ effect would dominate. Taking into account a high signal/noise ratio requirement, well established laser technology and the current use of 10 ns excitation in most airborne LIDAR fluorosensors, this pulse duration seems to be an optimal solution for conducting airborne P&P measurements.

A decay in the pump-induced fraction of carotenoid molecules in the triplet state explains the fast initial $(\Phi_F - \Phi_o)/\Phi_F$ rise over a few-μs scale in Figure 5. The lifetime of the carotenoid triplet state

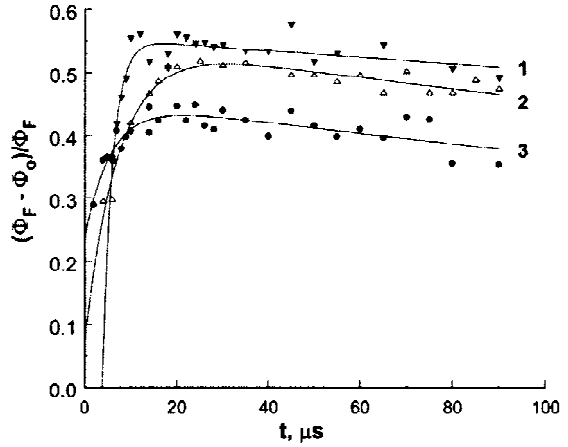

Figure 5. Examples of the relative change in fluorescence yield, $(\Phi_F - \Phi_o)/\Phi_F$, plotted as a function of delay, t, between the pump and probe pulses in the pump-probe pair ('P&P vs. Delay' protocol). Measurements obtained from *T. weissflogii* (1, 3) and *P. carterae* (2), are shown as discrete points. The solid curves represent results of non-linear regression of the points with Equation (16).

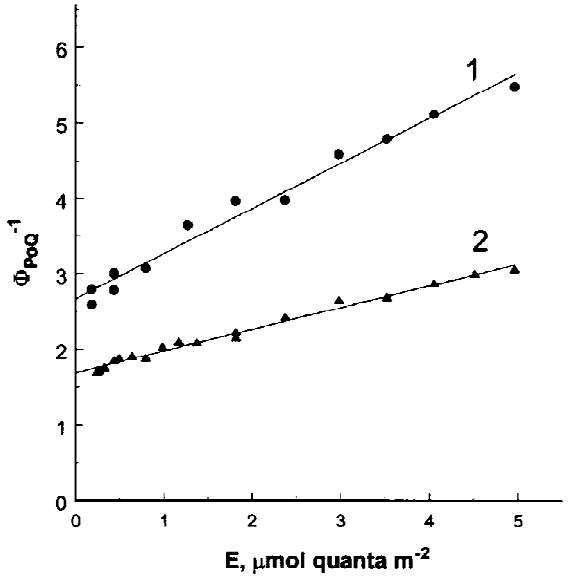

Figure 6. Examples of linear regression fitting (solid lines) of the reciprocal of the relative change in Chl fluorescence yield, ${\Phi_{PoQ}}^{-1}$ (discrete points), plotted as a function of probe pulse fluence, E, varied within the PS II sub-saturating range. 1: *P. carterae,* 2: *T. weissflogii*.

τ_T was found to be in the 4–7 μs range ('P&P vs. Delay' column of Table 1), which is consistent with earlier observations (e.g. Mathis et al. 1979; Breton et al. 1979). Based on these data, the optimal delay time between pulses in the pump-probe pair can be specified as $t = 2 \ln 10 \tau_T \cong 30\,\mu$s (see Equation (16)) both for phytoplankton and leaves of higher plants, which is consistent with results on leaves in Chekalyuk and Gorbunov (1995). The Φ_{Po} underestimation caused by the partial reopening of pump-closed RC's over this time is 3–7% based on the 0.4–1 ms τ_{A-} range estimated from 'P&P vs. Delay' measurements. The use of a longer pump-probe delay may result in a more significant underestimation of Φ_{Po} because of reopening of a higher fraction of pump-closed RC's (see the gradual decline in $(\Phi_F - \Phi_o)/\Phi_F$ at $t > 30\mu$s in Figure 5).

The σ_{PSII} estimates obtained within the phytoplankton groups studied ('P&P vs. Pump' column of Table 1) do not show a wide range of variation (25%), although the physiological state of the samples ranged from very poor to very good (Φ_P = 0.16..0.6). Furthermore, no significant differentiation was found between species in the group used in our investigation. The absolute σ_{PSII} values found in our laboratory study are consistent with those presented in the literature, i.e. 10^{-14}–10^{-13} cm^2 (e.g. see Dubinsky et al. 1986; Greene et al. 1992; Kolber et al. 1998). Somewhat lower σ_{PSII} values from our investigation (for instance, $8..12 \cdot 10^{-15}$ cm^2 in our experiment vs. $14..16 \cdot 10^{-15}$ in Dubinsky et al. (1986) for *T. weissflogii*) can be explained by less efficient absorption at the excitation wavelength of 532 nm used in our experiment, as well as stronger EEQ due to increased SSQ resulting from a short 8.5-ns pulse excitation.

For leaves of *Fagus grandifolia*, the E_s magnitude was found to be 4 times higher than for phytoplankton. This finding is consistent with the earlier measurements Chekalyuk and Gorbunov (1995) on leaves of maize, wheat and oak, and can be used along with the magnitude of the EEQ relative rate parameter R_Q (Table 1) for development of protocol for airborne measurement of photochemical activity in higher plants. More specific details on P&P measurements of plant leaves can be found in Chekalyuk and Gorbunov (1995). Taking average σ_{PSII} values obtained and using formula $E_s = 4.6{\sigma_{PSII}}^{-1}$ (see section 'Pump-and-probe technique'), the magnitude of the PS II saturating fluence can be specified as 10 μmol quanta m^{-2} (0.2 mJ/cm^2 at 532 nm) for phytoplankton and 40 μmol quanta m^{-2} (0.9 mJ/cm^2) for leaves of higher plants. Both the σ_{PSII} and E_s estimates are valid for the 532-nm excitation wavelength used in our laboratory investigations. A correction for wavelength dependence of PS II light absorption must be applied to adjust these estimates if a different excitation wavelength is used.

The EEQ data shows a potential feasibility for implementation of low-EEQ laser protocol based on fast repetition rate excitation (Falkowski and Kolber 1995; Kolber et al. 1998). The total fluence in the pulse burst must be E_s in magnitude to fully saturate PS II photochemistry over its 100 μs duration. The maximum pulse repetition rate achievable with advanced diode-pump solid state laser is about 100 kHz, which would result in a 10-pulse burst at an individual pulse fluence of $E_s/10$. At a 100 ns pulse duration, typical for 100 kHz laser, the SSQ effect would be negligible relative to the STQ effect as discussed above. Therefore, the EEQ quenching factor for an individual burst pulse would be in a range of 1.02–1.06 for the phytoplankton samples examined in our study. This estimate is based on Equation (14), $E_s = 4.6 \cdot {\sigma_{PSII}}^{-1}$, σ_{PSII} and 0.5 R_{STQ} data from Table 1. Further progress in laser technology may make the development of an airborne non-EEQ fast-repetition-rate LIDAR system feasible in the near future.

Based on the experimental results, the actual sensitivity advantage of the SP-P&P protocol over the 'weak-pulse' P&P protocol can be estimated. The product of the excitation fluence, the absorption cross-section and the fluorescence yield determines the magnitude of the fluorescence response from a unit excitation area in the water column. Assuming absorption is unchanged and EEQ is negligible at a 'weak-probe' fluence, $E_s/500$, the relative increase in fluorescence response in the EEQ mode (fluence E) compared to a 'weak-pulse' P&P can be estimated as $500\ E/E_s/Q_E$. For example, assuming the use of a 10 ns probe pulse with a PS II saturating fluence $E = E_s$ and $f = 0.5$ and $R_Q = 0.7$ for seawater and using the above estimate $Q_E(E_s) = 2.8$, the expected fluorescence increase would be $500/Q_E \cong 150$ times. Considering 0.3–0.6 as a typical phytoplankton range of PS II photochemical efficiency (Falkowski and Kolber 1995), the corresponding fluorescence parameter $\Phi_{PoQ} = \Phi_{Po}/Q_E(E_s)$ (see Equation (14)) would be in a range of 0.1–0.2, and could be, therefore, accurately measured from the airborne platform.

Conclusion

Thus, the SP-P&P protocol can provide a significant advantage in sensitivity, which is critical for an airborne implementation of the P&P concept and other low-signal applications, such as single-cell microscopy and flow cytometry. In practice, the operational probe pulse energy must be optimized within the PS II sub-saturating range to provide the best signal/noise ratio for a remotely measured Φ_{PoQ} fluorescent parameter. This parameter must be corrected for EEQ to assess the 'unquenched' magnitude of the PS II photochemical characteristics. The correction procedure (see Equation (15)) requires information about the relative EEQ rate, $R_Q E$, which was found to be independent of the PS II photochemical efficiency. Spatial and temporal changes in species composition can potentially result in a few-fold variability of the EEQ relative rate parameter, R_Q, according to our laboratory study. Changes in the flight altitude and beam propagation through the atmosphere and water can affect the excitation fluence E. Thus, the airborne measuring protocol should provide continuous $R_Q \cdot E$ monitoring for use in providing an EEQ correction.

Our recent airborne implementation of the SP-P&P protocol, its verification and optimization during the airborne field campaign (spring 1999) is discussed in detail in a subsequent paper (Chekalyuk et al. 2000). The basic idea is illustrated in the right panel in Figure 1. In short, the proposed protocol involves simultaneous measurements of the dependencies of the variable fluorescence and the pump-induced Chl fluorescence on the pump fluence, E_{pm}, which is varied pulse–pulse within the PS II sub-saturating range. During this procedure, the probe pulse fluence is fixed at a sub-saturating level, E, ensuring an optimal signal-to-noise ratio in the pump-induced fluorescence rise. The measurement of the pump-induced Chl fluorescence (unfilled triangle in the right panel in Figure 1) provides information to apply an EEQ data correction and retrieve PS II photochemical characteristics Φ_{po} and σ_{PSII}.

Acknowledgements

The authors would like to thank Prof. Paul Falkowski, Dr Zbigniew Kolber, and Dr Maxim Gorbunov for useful discussions and comments. The authors also thank Dr David Kramer and Dr Mark Williams for comments on the manuscripts, Marnie Zirbel for help in cultivating phytoplankton cultures, and Earl Frederick for providing leaves of *Fagus grandifolia* for laboratory experiments. We are grateful for the support of Dr Janet Campbell and Dr John Marra, former and current Ocean Biology Program Scientists at NASA Headquarters. Dr Alexander Chekalyuk is supported by an award from National Research Council (USA).

References

Breton J, Geacintov NE and Swenberg CE (1979) Quenching of fluorescence by triplet excited states in chloroplasts. Biochim Biophys Acta 548: 616–635

Bunin DK, Gorbunov MYu, Fadeev VV and Chekalyuk AM (1992) Emission of fluorescence from chlorophyll *a in vivo* due to nanosecond pulsed laser excitation. Sov J Quantum Electron 22: 381–383

Chekalyuk AM and Gorbunov MYu (1994) Pump-and-probe LIDAR fluorosensor and its applications for estimates of phytoplankton photosynthetic activity. In: Second Thematic Conference on Remote Sensing for Marine and Coastal Environments, pp 389–400. New Orleans, USA, 31 January – 2 February 1994

Chekalyuk AM and Gorbunov MYu (1995) Development of the LIDAR pump-and-probe technique for remote measuring the efficiency of primary photochemical reactions in leaves of green plants. EARSeL Advances in Remote Sensing 3: 42–56

Chekalyuk AM, Demidov AA, Fadeev VV and Gorbunov MYu (1995) Lidar monitoring of phytoplankton and dissolved organic matter in the inner seas of Europe. EARSeL Advances in Remote Sensing 3: 131–139

Chekalyuk AM, Olson RJ and Sosik HM (1997) Pump-during-probe fluorometry of phytoplankton: Group-specific photosynthetic characteristics from individual cell analysis. Proc SPIE 2963: 840–845

Chekalyuk AM, Hoge FE, Wright CW, Swift RN and Yungel JK (2000) Airborne test of laser pump-and-probe technique for assessment of phytoplankton photochemical characteristics. Photosynth Res 66: 45–56 (this issue)

Deprez J, Dobek A, Geacintov NE, Pailotin G and Breton J (1983) Probing fluorescence induction in chloroplasts on a nanosecond time scale utilizing picosecond laser pulse pairs. Biochim Biophys Acta 725: 444–454

Dubinsky Z, Falkowski PG and Wyman K (1986) Light harvesting and utilization by phytoplankton. Plant Cell Physiol 27: 1335–1349

Falkowski PG and Kolber Z (1995) Variations in chlorophyll fluorescence yields in phytoplankton in the world oceans. Aust J Plant Physiol 22: 341–355

Falkowski PG, Fujita Y, Ley A and Mauzerall D (1986) Evidence for cyclic electron flow around Photosystem II in *Chlorella pyrenoidosa*. Plant Physiol 81: 310–312

Falkowski PG, Greene R and Geider R (1992) Physiological limitations on phytoplankton productivity in the ocean. Oceanography 5: 84–91

Genty B, Briantis J-M and Baker N (1989) The relationship between the quantum yield of photosynthetic electron transport and quenching of chlorophyll fluorescence. Biochim Biophys Acta 990: 87–92

Govindjee (1995) Sixty-three years since Kautski: Chlorophyll *a* fluorescence. Aust J Plant Physiol 22: 131–160

Greene R, Geider R, Kolber Z and Falkowski PG (1992) Iron-induced changes in light harvesting and photochemical energy conversion processes in eukaryotic marine algae. Plant Physiol 100: 565–575

Guillard RRL (1975) Culture of phytoplankton for feeding marine invertebrates. In: Smith WL and Chanley (eds) Culture of Marine Invertebrate Animals, pp 29–60. Plenum Publishing Corp, New York

Hofstraat JW, Peters JCH and Geel C (1994) Simple determination of photosynthetic efficiency and photoinhibition of *Dunaliella tertiolecta* by saturating pulse fluorescence measurements. Mar Ecol Prog Ser 103: 187–196

Hoge FE (1988) Oceanic and terrestrial lidar measurements. In: Measures RM (ed) Laser Remote Chemical Analysis, pp 409–503. John Wiley and Sons, New York

Hoge FE, Wright CW, Lyon PE, Swift RN and Yungel JK (1999) Satellite retrieval of inherent optical properties by inversion of an oceanic radiance model: A preliminary algorithm. Appl Opt 38: 495–504

Johnson B, Higgs C, Primmerman C, Mandra R, Jeys T, DeFeo W, Grey P and Rowe G (1995) Airborne LIDAR measurements of phytoplankton abundance and productivity in New England coastal waters. In: Third Thematic Conference on Remote Sensing for Marine and Coastal Environments, pp 819–832. Seattle, Washington, 18–20 September 1995

Karukstis KK, Boegemen SC, Fruetel JA, Gruber SM and Terris MH (1987) Multivariate analysis of Photosystem II fluorescence quenching by substituted benzoquinones and naphthoquinones. Biochim Biophys Acta 891: 256–264

Kim HH (1973) New algae mapping technique by the use of an airborne laser fluorosensor. Appl Opt 12: 1454–1459

Kolber Z, Prazil O and Falkowski PG (1998) Measurements of variable chlorophyll fluorescence using fast repetition rate techniques: Defining methodology and experimental protocols. Biochim Biophys Acta 1367: 88–106

Kramer DM and Crofts AR (1996) Control and measurement of photosynthetic electron transport *in vivo*. In: Baker N (ed) Photosynthesis and the Environment, pp 25–66. Kluwer Academic Publishers, Dordrecht, The Netherlands

Kramer DM, Robinson HR and Crofts AR (1990) A portable multiflash kinetic fluorimeter for measurement of donor and acceptor reactions of Photosystem 2 in leaves of intact plants under filed conditions. Photosynth Res 26: 181–193

Krause GH and Weis E (1991) Chlorophyll fluorescence and photosynthesis: the basics. Annu Rev Plant Physiol Plant Mol Biol 42: 313–349

Mathis P, Butler WL and Satoh K (1979) Carotenoid triplet state and chlorophyll fluorescence quenching in chloroplasts and subchloroplast particles. Photochem Photobiol 30: 603–614

Mauzerall D (1972) Light-induced fluorescence changes in *Chlorella*, and the primary photoreactions for production of oxygen. Proc Natl Acad Sci 69: 1358–1362

Olson RJ, Chekalyuk AM and Sosik HM (1996) Phytoplankton photosynthetic characteristics from fluorescence induction assays of individual cells. Limnol Oceanogr 41: 1253–1263

Olson RJ, Sosik HM and Chekalyuk AM (1999) Photosynthetic characteristics of marine phytoplankton from pump-during-probe fluorometry of individual cells at sea. Cytometry 37: 1–13

Rosema A and Zahn H (1997) Laser pulse energy requirements for remote sensing of chlorophyll fluorescence. Remote Sens Environ 62: 101–108

Schlodder E, Brettel K, Schatz GH and Witt HT (1984) Analysis of the Chl-$a_{II}{}^{+}$ reduction kinetics with nanosecond time resolution in oxygen-evolving Photosystem II particles from *synechococcus* at 680 and 824 nm. Biochim Biophys Acta 765: 178–185

Schreiber U, Neubauer C and Schliwa U (1993) PAM fluorometer based on medium-frequency pulsed Xe-flash measuring light: A highly sensitive new tool in basic and applied photosynthesis research. Photosynth Res 36: 65–72

Vulkunas L, Geacintov NE, France L and Breton J (1991) The dependence of the shapes of fluorescence induction curves in chloroplasts on the duration of illumination pulses. Biophys J 59: 397–408